Torque Improvement of a Dual Rotor Coreless Axial Flux-Switching Generator for High Speed Wind Turbine

Omid Aghapour[1], Milad Niaz Azari[1*], Seyyed Mehdi Mirimani[2]

***Abstract*-- Coreless axial flux permanent magnet (PM) machines (AFPM) have attracted significant interest over the last decades as an ideal candidate for a wide range of applications. This is generally due to their advantages, such as the high torque density, high power density, and the light weight. This paper investigates the performance of a coreless axial flux-switching generator (AFSMG) with improved torque characteristics. The inherent feature of the axial flux-switching machines is the high cogging torque. Hence the main advantage and the novelty of this research is addressing a suitable key for its torque characteristics challenges. In this regard, a comprehensive study is done on rotor tooth shape. First, the geometry and the shape of the rotor tooth are optimized, and then the skewing technique is applied to minimize the cogging torque and improve the total harmonic distortion. Finally, the cogging torque and the THD are calculated in the primary design and the optimal design. The Taguchi method is utilized to improve the primary model. A comparative analysis of the primary and optimized model is carried out, which indicates the better performance of the optimized design. Furthermore, the 3D finite element method is applied to verify the results of the presented model.**

***Index Terms*-- AC Generators, Coreless Axial Flux Machines, Taguchi Methods.**

I. INTRODUCTION

Different structures of axial flux machines have been comprehensively investigated over the last decade, and this is due to their unique features such as high power density, compact structure, lightweight, and high efficiency [1-3]. Among these various topologies, coreless axial flux machines have attracted great interest. Hence, these machines are studied and investigated comprehensively to obtain higher torque density, higher efficiency, and lower weight. Furthermore, a number of studies have been focused on the enhancement of the mean value of their electromagnetic torque [4-7]. These studies were useful and applicable to improve the performance of the coreless axial flux machines. However, the design process that is introduced in these papers has led to more complexity and difficulty in manufacturing these structures. Hence, an optimum solution should be presented to mitigate these problems and improve the efficiency and performance of the machines.

Axial flux-switching permanent magnet (AFSPM) machine is a novel permanent magnet (PM) machine consisting of PM and coil on the stator and no windings or permanent magnets on the rotor. High power density, high efficiency, sinusoidal waveform back-EMF, flux weakening capability, and favorable cooling are the advantages of this type of machine [8], [9]. However, because of the doubly salient construction and the high amount of flux density caused by the flux-focusing effects, the cogging torque of the AFSPM machine is higher than the classical PM one.

In comparison with the slotted type of AFPM machines, the coreless stator brings additional advantages because, by eliminating the stator core, iron losses are removed from the machine. Elimination of cogging torque, higher motor efficiency, and the smaller motor stack are other advantages of coreless type AFPM machines [10, 11, 12]. However, it has to be considered that the PM rule in coreless construction is more than that of the cored model due to greater electrical air gaps to achieve the same magnetic air-gap flux density. In addition to the above benefits, cogging torque is also eliminated in coreless AFPM motors due to the absence of core material and reluctance variation.

Innovative structures of the coreless axial flux-switching machine are presented in [13-15]. But the biggest challenge of these topologies is related to their high peak amount of cogging torque, which leads to high noise and vibration of the machine. Furthermore, it affects the performance of the motor in the starting and running regimes. Hence, these structures were not designed optimally and were not presented with an appropriate solution to mitigate the peak value of the cogging torque. The proposed axial flux-switching permanent magnet generator discussed in this paper is shown in Fig. 1. As can be seen, the stator of this generator is coreless and consists of coils and permanent magnets. From the view of the application of this type of machine, they can be used in wind turbines [16]. In summary, coreless axial flux-switching machines offer specific merits. which can be stated as follows:

- Simplified stator core
- Reduced axial size compared to the cored one
- Low prototyping cost due to use of the epoxy resin
- Robust rotor structure

In this paper, the rotor tooth structure of an axial flux-switching machine is investigated, which can extremely affect the performance of the generator. Consequently, this research will

1- Department of Electrical Engineering University of Science and Technology of Mazandaran Behshahr, Iran.
Corresponding author: miladniazazari@mazust.ac.ir

2- Elctrical and Computer Engineering Department Babol Noshirvani University of Technology Babol, Iran.

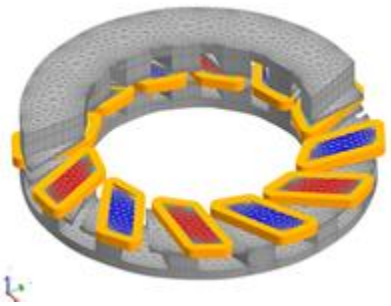

Fig. 1: Studied AFSPM

mainly focus on the optimal design of the rotor topology to decrease the peak value of cogging torque as well as the THD. In this regard, a comprehensive study is carried out on the optimal design of the rotor geometry. In the next section, the configuration and principles of the proposed coreless axial flux-switching machine are introduced. In Section III, the sizing equations and the design process are outlined. Then, the skewing technique is applied to this structure, and the optimum skew angle is determined by the Taguchi method. Although the skewing technique was applied in other research and it's a well-known method [17], in this paper it's applied on the rotor teeth of the proposed generator. Finally, the performance of the optimized model is compared with the primary generator in terms of the cogging torque and the THD in Section IV.

II. CONFIGURATION AND PRINCIPLES OF GENERATOR PERFORMANCE

A. Proposed generator

Fig. 2a illustrates a 3D perspective of the stator. As can be observed, the stator is coreless and constructed of epoxy resin. Furthermore, it is made up of 14 identical PMs that are encircled by trapezoidal coils. In these structures, rare-earth magnets are used to provide increased flux density. These magnets are arranged circumferentially to provide the machine's required flux density. Rotors, as illustrated in Fig. 2b, have 14 teeth and are designed to reduce cogging torque and torque ripple. On the other hand, skewing is done to offset the slot effects, which results in an improvement in the torque profile.

B. Generator performance

Fig. 3 illustrates the performance of the generator in a complete cycle. According to the position of the magnets and rotor teeth, different flux paths are created, which cause various values of EMF at any given time. Initially, in Fig. 3b, the stator poles and rotors teeth are fully aligned, which leads to the maximum EMF value. As the rotor rotate, in Fig. 3c, each magnet is located against the space between two rotor teeth. Hence the value of EMF decreases. When the generator is running, this cycle is repeated to produce a sinusoidal flux and the resulting EMF.

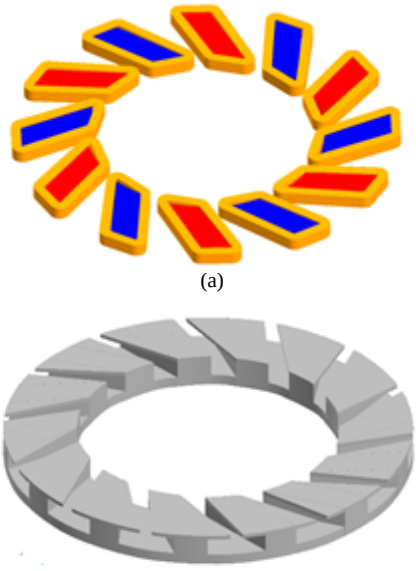

(a)

(b)

Fig. 2. a) Coreless Stator b) Salient Rotor

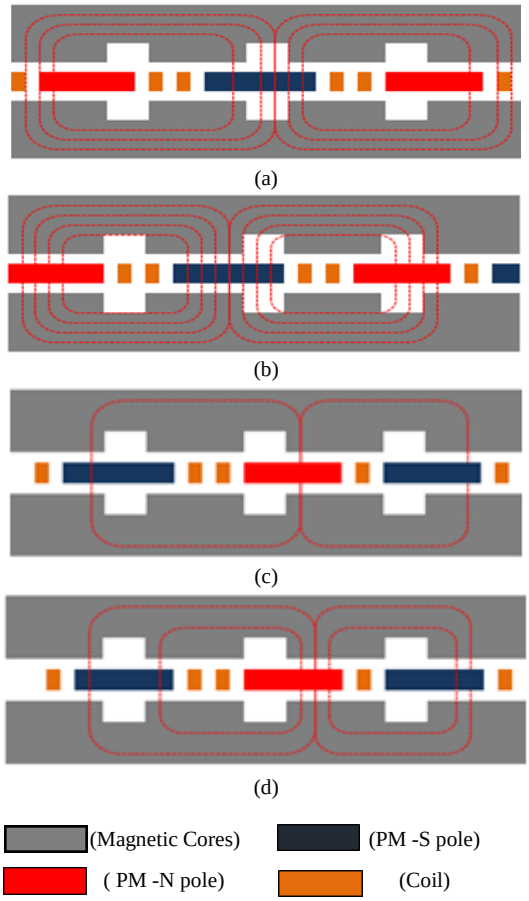

Fig. 3. Flux distribution of the proposed generator at different rotor position in the complete cycle

III. DESIGN PROCESS OF THE PROPOSED MODEL

In this section, the design process of the proposed generator is discussed. After introducing fundamental sizing equations, the geometry of the primary generator is derived from the results of these equations. In order to improve the performance of the proposed model, an optimization is carried out on the shape of the teeth as well as skewing them.

A. Sizing Equations

Sizing equations play an important role in determining the dimensions of the generator. So, in this section, the geometry of the machine is obtained by these equations. According to [18, 19], the output power of the generator can be obtained as follows:

$$p_{out} = \eta \frac{m}{T} \int_0^T e(t).i(t)d = mk_p \eta E_{PK} I_{PK} \quad (1)$$

Where η is the efficiency, m is the number of machine phases, E_{PK} is peak of the EMF values, and $e(t)$ represents the induction voltage value, and T, $i(t)$, k_p, I_{PK} are period of the induction voltage, phase current, waveform factor of the power, and peak of the phase current, respectively. Also k_p can be obtained by:

$$k_p = \frac{1}{T} \int_0^T \frac{e(t).i(t)}{E_{pk} I_{pk}} dt \quad (2)$$

The induced voltage is obtained by:

$$E_P = 4.44 f N_{ph} \phi_{pole} \quad (3)$$

Where f is the output frequency, N_{ph} is the number of coil turns per phase, and ϕ_{pole} is the airgap magnetic flux per pole can be obtained by:

$$\varphi_{pole} = B_{mg} \alpha_p = B_{mg} \alpha_P \frac{\pi}{8N_r} (1 - \lambda^2) D_o \quad (4)$$

Where α_p, N_r, λ are the magnet width to pole pitch ratio, the number of rotor teeth, and the generator inner to outer diameter ratio, respectively. Also D_O is outer diameter of the machine can be obtained from (5):

$$D_{out} = \sqrt[3]{\frac{32 P_{out}}{\pi^3 \alpha_p K_W w_s B_{mg} (1 - \lambda^2)(1 + \lambda) \cos \varphi}} \quad (5)$$

Where K_w is the winding factor coefficient and w_s is the rotor speed. The peak value of the phase current can be calculated by:

$$I_{pk} = \frac{A\pi(1 + \lambda)}{4mN_{ph}} D_o K_i \quad (6)$$

Where A is the machine electrical loading, and the number of machine phases is m , also k_i can be calculated from (7):

$$k_i = \frac{I_{pk}}{I_{rms}} = \frac{1}{\sqrt{\frac{1}{T} \int_0^T \left(\frac{i_{(t)}}{I_{pk}} \right)^2 dt}} \quad (7)$$

Where I_{rms} represensts the effective voltage value. The electromagnetic torque of the machine can be as below:

$$T = F_x R_{in} = 2\pi B_{av} A (R_O^2 - R_{in}^2) R_{in} \quad (8)$$

Where R_O and R_{in} are the outer and inner radius of the machine respectively.

B. Sensitivity analysis and enhancement of the proposed generator

Cogging torque and torque ripple are minimized to improve the performance of the machine, which plays a crucial role in the decline of the noise and the vibration of the generator. The proposed model is designed in a way to tackle these challenges. The structure of the rotor teeth can highly affect the performance of the generator. Hence, these must be designed optimally to achieve the sinusoidal EMF. The main parameters of the AFSPM generator are illustrated in Table I.

In this research, rotor tooth design and teeth skewing technique are carried out to improve the performance of the proposed machine. Furthermore, magnetic flux saturation is considered in this paper to design an optimal topology. In Fig. 4, the improved model of the rotor teeth is shown.

TABLE I
Main Parameters of the AFSPM Generator

Description	Symbol	Unit	Value
Rated Power	p_{out}	w	1000
Rated Speed	W_s	rpm	1500
No. of phases	m	--	3
No. of turn per phase	N_{ph}	--	260
Number of rotor tooth	N_r	--	28
Number of stator coils	Q_c	--	12
Outer diameter	D_o	mm	270
Air gap Length	L_g	mm	1.5
Ratio of inner to outer diameter	λ	--	0.7
Back iron	B_i	mm	8
Tooth length	T_l	mm	50
Tooth width	T_{w_1}	mm	14
Tooth height	T_{h_1}	mm	13

As can be seen, the size of the rotor teeth has been calculated. Sensitivity analysis is used to study the effect of rotor tooth geometry on generator output and to choose the optimal combination of rotor tooth geometry and skew angle. The suggested model's performance is optimized and improved by selecting total harmonic distortion (THD) and cogging torque

as goal functions. The steps of the optimization approach are listed in the next paragraph:

First, according to the topology of the proposed generator, a number of variables are chosen as follows: T_{w_1}, T_{w_2}, T_h, and θ_s, which are shown in Fig. 4.

After that, in order to determine the optimum combination of these parameters, the Taguchi method is applied. This optimization method uses an orthogonal array to find the best combination of the variables. Accordingly, five levels, are defined for each parameter. According to these variables and their corresponding levels an orthogonal array is defined, which is shown in Table II. It consists of 25 experiments. Each experiment introduces a unique combination of variables and their levels. FEM simulations are carried out according to these 25 scenarios. In each experiment, the outputs of the generator, such as the cogging torque and the THD are achieved.

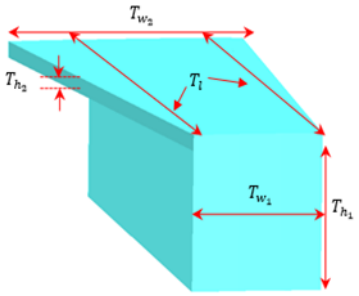

Fig. 4. Optimal rotor tooth topology

TABLE II

L25 Orthogonal Array

Experiment no	T_{w_1}	T_{h_1}	T_{w_2}	θ_s
1	1	1	1	1
2	1	2	2	2
3	1	3	3	3
4	1	4	4	4
5	1	5	5	5
6	2	1	2	3
7	2	2	3	4
8	2	3	4	5
9	2	4	5	1
10	2	5	1	2
11	3	1	3	5
12	3	2	4	1
13	3	3	5	2
14	3	4	1	3
15	3	5	2	4
16	4	1	4	2
17	4	2	5	3
18	4	3	1	4
19	4	4	2	5
20	4	5	3	1
21	5	1	5	4
22	5	2	1	5
23	5	3	2	1
24	5	4	3	2
25	5	5	4	3

The average effect is calculated to determine the optimum combination of the control variables. For this proposed, the mean value of i_{th} level can be obtained from equation (9):

$$Average\ Effect = \frac{1}{n}\sum_{i=1}^{n} X_i \tag{9}$$

Where n and X are the number of scenarios and the corresponding ith level of the proposed factor. The average effect of each variable on the THD and cogging torque is shown in Figs. 5 and 6 respectively. As can be seen, $\theta_s$and T_{w_2} have the major influence on the THD and the cogging torque, while T_{w_1} has the lowest impact on the THD. On the other hand, T_{h_1} and has the significant effect on the cogging torque and the least impact on the THD.

IV. PERFORMANCE ANALYSIS OF THE IMPROVED MODE

In this section, the results of the finite element method (FEM) simulation of the proposed machine are presented. The outputs of the optimized and primary generator, such as cogging torque, EMF, and output torque, are presented and compared.

A. Flux distribution at no load

In the proposed generator, the only source for producing flux density are magnets. Fig. 7 shows the flux linkage of the optimized model at nominal speed. As can be seen, the maximum amount of flux linkage in this structure is in the yoke and corner of the rotor teeth, which are normal amounts of flux density for the specific material.

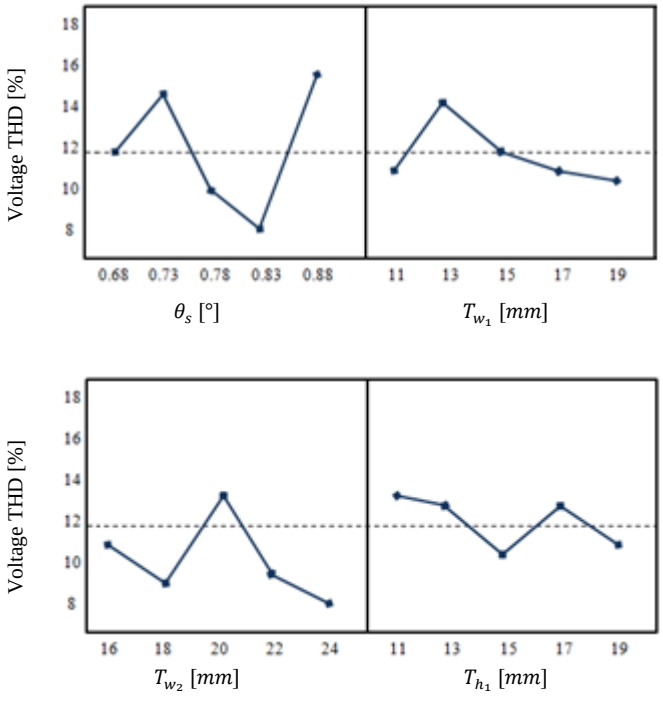

Fig. 5. Mean effect of optimization variable on the phase voltage total harmonic distortion

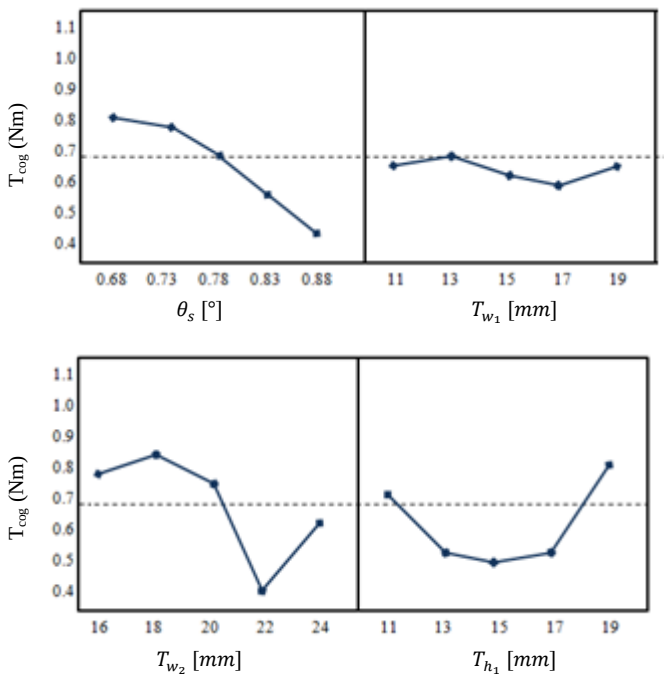

Fig. 6. Mean effect of optimization variables on the cogging torque

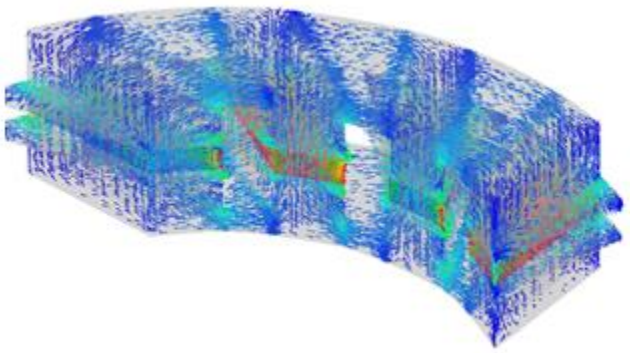

Fig 7. No-load flux distribution of the magnets in optimized model

B. *EMF and harmonic spectrums*

According to the results of the Taguchi optimization method, the optimum geometry of the optimized topology is obtained. With respect to these results, the EMF of the optimized and primary machine is compared in this section. Fig. 8 illustrates the EMF of the initial and optimal design at the rated speed (1500). As can be seen, the peak of the EMF value for the optimized model is higher than the primary one. Also, the waveform of the final model is more symmetrical compared with the primary generator, and this is due to the lower THD of the optimized machine. Fig. 9 shows the harmonic spectrums of the improved and primary models. As can be seen, the THD of the voltage is approximately 13% in the primary design, while this amount is only 3.7% in the improved one.

C. *Cogging torque and output torque*

Cogging torque is a torque profile problem in the design process of the proposed model, resulting in significant acoustic noise and vibration of the machine, as well as high torque ripple. Torque ripple causes speed variations and makes it difficult to start a machine at low speeds. The suggested model has a significant cogging torque due to the rotors' distinct structure. As a result, sensitivity analysis and tooth skewing are performed to reduce the irritating torque profile. Fig. 10 depicts the peak-to-peak value of the cogging torque of the original and enhanced generators. As can be observed, the highest value of the cogging torque decreased dramatically from 1.2 N.M, which is about 20% of the mean torque, to approximately 0.3 N.M., which is 4% of the average torque. This drop is mostly due to the optimum design of the rotor teeth and the skewing process.

Fig. 11 shows the full load torque of the primary and optimal design of the proposed model. As can be seen, the mean torque of the primary generator is equal to 6.36 N.M, while this amount is 5.9 N.M. for the improved model. The reduction of the average torque of the improved model is due to the decline of the amount of torque ripple by approximately 30% compared with the initial design.

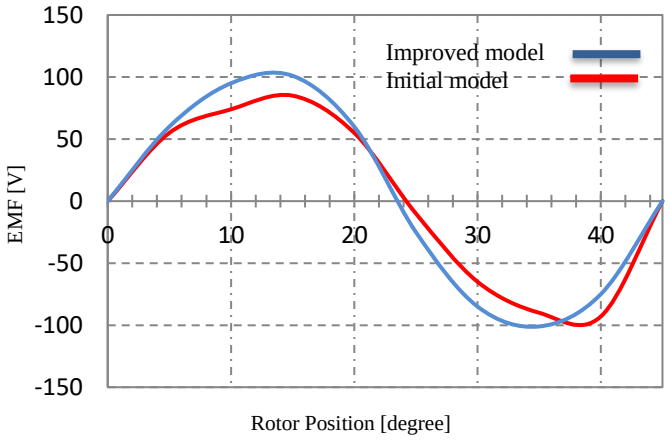

Fig. 8. EMF waveform of the primary and optimized generator

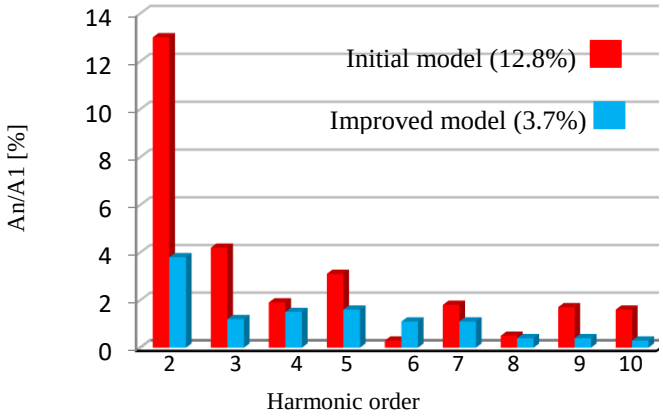

Fig. 9. EMF harmonic components of the initial and finally design

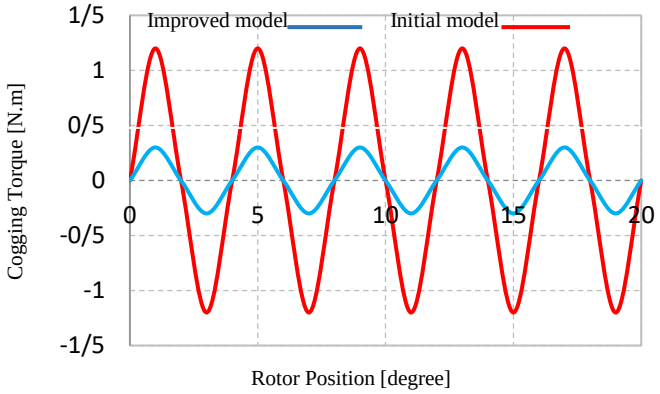

Fig. 10. Cogging torque of the primary and optimized model

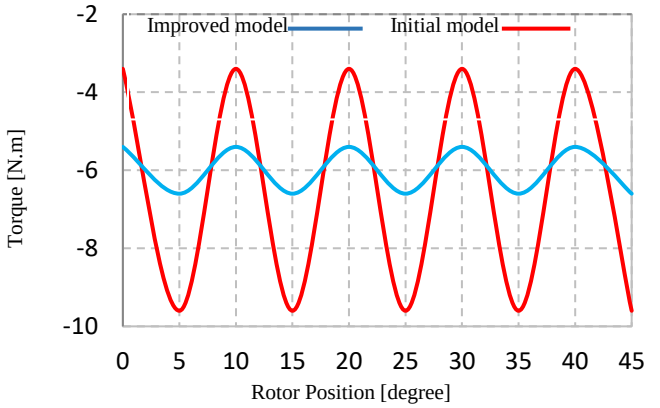

Fig. 11. Full load torque of the initial and optimized design

V. CONCLUSION

In this research, an optimal structure of a coreless axial flux switching machine is presented, and the performance of this machine is analyzed. Furthermore, the main challenge of the design process of these kinds of machines, such as high cogging torque and THD, is investigated. After that, by the taguchi optimization method and skewing rotor teeth, the structure of the machine was optimized. Finally, the performance of the primary and optimized generators is compared, which shows the better performance of the improved model in terms of the peak-to-peak value of the cogging torque and the THD. It should be stated that, THD decreased by about 16% in the optimized machine.

REFERENCES

[1] A. Mahmoudi, S. Kahourzade, N. A. Rahim, W. P. Hew and M. N. Uddin , "Design and prototyping of an optimised axial-flux permanent-magnet synchronous machine," *IET Electric Power Application*, vol. 7, no. 5, pp. 338-349, 2013.

[2] S. Kahourzade, A. Mahmoudi, H. W. Ping, et al, "A comprehensive review of axial-flux permanent-magnet machines," Can J. Electro. Comput. Eng, no. 19-33, p. 37, 2014.

[3] Maarten J. Kamper, Rong-Jie Wang, Francois G. Rossouw, "Analysis and Performance of Axial Flux Permanent-Magnet Machine With Air-Cored Nonoverlapping Concentrated Stator Windings," IEEE Transactions on Industry Applications , vol. 44, no. 5, pp. 1495 - 1504, 2008.

[4] P. Hekmati, M. Mirsalim, "Design and Analysis of a Novel Axial-Flux Slotless Limited-Angle Torque Motor With Trapezoidal Cross Section for the Stator," IEEE Transactions on Energy Conversion, vol. 28, no. 4, pp. 815 - 822, 2013.

[5] Reza Mirzahosseini, Ahmad Darabi, Mohsen Assili, "Magnet shifting for back EMF improvement and torque ripple reduction of a TORUS-type nonslotted axial flux permanent magnet machine," International Transactions on Electrical Enegy Systems, vol. 30, no. 4, 2019.

[6] M. Aydin, M. Gulec, "Reduction of Cogging Torque in Double-Rotor Axial-Flux Permanent-Magnet Disk Motors: A Review of Cost-Effective Magnet-Skewing Techniques With Experimental Verification," IEEE Transactions on Industrial Electronics, vol. 61, no. 9, pp. 5025 - 5034, 2014.

[7] M. Gulec, M. Aydin, "Magnet asymmetry in reduction of cogging torque for integer slot axial flux permanent magnet motors," IET Electric Power Applications , vol. 8, no. 5, p. 189 – 198, 2014.

[8] J.F. Gieras, I.A. Gieras, "Performance analysis of a coreless permanent magnet brushless motor," in 37th IAS Annual Meeting (Cat. No.02CH37344), Pittsburgh, 2002.

[9] M. J. Kamper, W. R. Jie, and F. G. Rossouw, "Analysis and performance of axial flux permanent-magnet machine with air-cored nonoverlapping concentrated stator windings," IEEE Transaction on Industry Application, vol. 44, no. 5, pp. 1495-1504, 2008.

[10] Youlong Wang, Wen Xuhui Chen Chen, Zhang Dong, "A parametric magnetic network model for axial flux permanent magnet machine with coreless stator," in 17th International Conference on Electrical Machines and Systems (ICEMS), Hangzhou, China, 2014.

[11] J.R. Bumby, R. Martin, M.A Mueller, E. Spooner, N.L. Brown, B.J. Chalmers, "Electromagnetic design of axial-flux permanent magnet machines," IEE Proceedings - Electric Power Applications , vol. 151, no. 2, pp. 1350-2352, 2004.

[12] Roberto Di Stefano, Fabrizio Marignetti, "Electromagnetic Analysis of Axial-Flux Permanent Magnet Synchronous Machines With Fractional Windings With Experimental Validation," IEEE Transactions on Industrial Electronics, vol. 59, no. 6, pp. 2573 - 2582, 2012.

[13] Li Hao, Mingyao Lin, Da Xu, Nian Li, Wei Zhang, "Analysis of Cogging Torque Reduction Techniques in Axial-Field Flux-Switching Permanent-Magnet Machine," IEEE Transactions on Applied Superconductivity , vol. 26, no. 4, pp. 1051-8223, 2016.

[14] Yu Chen, Z. Q. Zhu, David Howe, "Three-Dimensional Lumped-Parameter Magnetic Circuit Analysis of Single-Phase Flux-Switching Permanent-Magnet Motor," IEEE Transactions on Industry Applications , vol. 44, no. 6, pp. 1701 - 1710, 2008.

[15] H. Asgharpour-Alamdari, "Design optimization of coreless stator axial flux-switching motor," Sci Iran, 2021.

[16] Dehshiri M, Ketabi A. "A coreless axial flux-switching generator for micro-wind turbine application" Energy Sci Eng. 2022; 10: 4804-4813. doi:10.1002/ese3.1309

[17] M. Aydin, "Magnet skew in cogging torque minimization of axial gap permanent magnet motors," in 18th International Conference on Electrical Machines, Vilamoura, Portugal, 2008.

[18] Surong Huang, Jian Luo, F. Leonardi, T.A. Lipo, "A general approach to sizing and power density equations for comparison of electrical machines," IEEE Transactions on Industry Applications, vol. 34, no. 1, pp. 92 - 97, 1998.

[19] Jacek F. Gieras , Rong-Jie Wang , Maarten J. Kamper, Axial Flux Permanent Magnet Brushless Machines, Netherlands: Springer, 2008.